Scientific report *on the implementation of project* ***PN-II-ID-PCE-2011-3-0868****; contract no.* ***264/2011***
Period: ***January – December 2012***

According to the project proposal, the following objectives have been solved in the phase I/2012 of this project:

O1/ Critical parameters determining the properties of metallic nanoparticles (NP) dispersed on mesoporous SBA-15 support by MDI method (Mild Drying Impregnation)

In the first phase of the project, samples of mesoporous silica of SBA-type were prepared having different textural properties (in particular, the diameter of primary mesopores and micropores volume)[1] as well as mesoporous aluminosilica of Al-SBA-15-type with different chemical compositions.[2] In the second phase, the calcined supports, stored in the absence of humidity, have been impregnated with aqueous solutions of the corresponding nitrates (by Incipient Wetness Impregnation method - IWI), followed by a drying stage in various conditions and finally calcination under the stagnant air conditions free from the "container effect"[3] (specifications are shown in Table 1). Optionally, after drying, some samples were reduced directly in a hydrogen flow.

Table 1. Sample summary of catalytic precursors (MO/SBA-15) prepared by MDI method.

Nr	Sample	Code	Type	Synthesis conditions/Thermal treatment
1	SBA-15	SBA-15[60]	Catalytic support	Hydrothermal treatment 60 °C, 48 h, calcination 550 °C, desiccator $CaCl_2$
2	NiO/SBA-15	5NiO/SBA-15[60]/ 25-5	Catalytic precursor	5wt.%, drying 25 °C, 5 days, calcination 500 °C
3	CuO/SBA-15	5CuO/SBA-15[60]/ 25-5		
4	Co_3O_4/SBA-15	5Co_3O_4/SBA-15[60]/ 25-5		
5	SBA-15	SBA-15[80]	Catalytic support	Hydrothermal treatment 80 °C, 48 h, calcination 550 °C, desiccator $CaCl_2$
6	NiO/SBA-15	5NiO/SBA-15[80]/ 25-5	Catalytic precursor	5wt.%, drying 25 °C, 5 days, calcination 500 °C
7	CuO/SBA-15	5CuO/SBA-15[80]/ 25-5		
8	Co_3O_4/SBA-15	5Co_3O_4/SBA-15[80]/ 25-5		
9	SBA-15	SBA-15[100]	Catalytic support	Hydrothermal treatment 100 °C, 48 h, calcination 550 °C, desiccator $CaCl_2$
10	NiO/SBA-15	5NiO/SBA-15[100]/ 25-2	Catalytic precursor	5wt.%, drying 25 °C, 2 zile, calcination 500 °C
11		5NiO/SBA-15[100]/ 25-5		5wt.%, drying 25 °C, 5 zile, calcination 500 °C
12		5NiO/SBA-15[100]/ 25-15		5wt.%, drying 25 °C, 15 zile, calcination 500 °C
13		5NiO/SBA-15[100]/ 25-30		5wt.%, drying 25 °C, 30 zile, calcination 500 °C
14		5NiO/SBA-15[100]/ 25-60		5wt.%, drying 25 °C, 60 zile, calcination 500 °C
15		5NiO/SBA-15[100]/ 25-150		5wt.%, drying 25 °C, 150 zile, calcination 500 °C
16		5NiO/SBA-15[100]/ 50-5		5wt.%, drying 50 °C, 5 zile, calcination 500 °C
17		5NiO/SBA-15[100]/ 100-5		5wt.%, drying 100 °C, 5 zile, calcination 500 °C
18		10NiO/SBA-15[100]/ 25-2		10wt.%, drying 25 °C, 2 zile, calcination 500 °C
19		10NiO/SBA-15[100]/ 25-5		10wt.%, drying 25 °C, 5 zile, calcination 500 °C
20		10NiO/SBA-15[100]/ 25-15		10wt.%, drying 25 °C, 15 zile, calcination 500 °C
21		10NiO/SBA-15[100]/ 25-30		10wt.%, drying 25 °C, 30 zile, calcination 500 °C
22		10NiO/SBA-15[100]/ 25-60		10wt.%, drying 25 °C, 60 zile, calcination 500 °C
23		10NiO/SBA-15[100]/ 25-150		10wt.%, drying 25 °C, 150 zile, calcination 500 °C
24	CuO/SBA-15	5CuO/SBA-15[100]/ 25-5	Catalytic precursor	5wt.%, drying 25 °C, 5 zile, calcination 500 °C
25		10CuO/SBA-15[100]/ 25-2		10wt.%, drying 25 °C, 2 zile, calcination 500 °C
26		10CuO/SBA-15[100]/ 25-5		10wt.%, drying 25 °C, 5 zile, calcination 500 °C
27		10CuO/SBA-15[100]/ 25-15		10wt.%, drying 25 °C, 15 zile, calcination 500 °C
28		10CuO/SBA-15[100]/ 25-30		10wt.%, drying 25 °C, 30 zile, calcination 500 °C
29		10CuO/SBA-15[100]/ 25-60		10wt.%, drying 25 °C, 60 zile, calcination 500 °C
30		10CuO/SBA-15[100]/ 25-150		10wt.%, drying 25 °C, 150 zile, calcination 500 °C
31		5CuO/SBA-15[100]/ 50-5		5wt.%, drying 50 °C, 5 zile, calcination 500 °C
32		5CuO/SBA-15[100]/ 100-5		5wt.%, drying 100 °C, 5 zile, calcination 500 °C
33	Co_3O_4/SBA-15	5Co_3O_4/SBA-15[100]/ 25-5	Catalytic precursor	5wt.%, drying 25 °C, 5 zile, calcination 500 °C
34		5Co_3O_4/SBA-15[100]/ 50-5		5wt.%, drying 50 °C, 5 zile, calcination 500 °C
35		5Co_3O_4/SBA-15[100]/ 100-5		5wt.%, drying 100 °C, 5 zile, calcination 500 °C
36		10Co_3O_4/SBA-15[100]/ 25-5		10wt.%, drying 25 °C, 5 zile, calcination 500 °C
37	SBA-15	SBA-15[120]	Catalytic support	Hydrothermal treatment 120 °C, 48 h, calcination 550 °C, desiccator $CaCl_2$
38	NiO/SBA-15	5NiO/SBA-15[120]/ 25-5	Catalytic precursor	5wt.%, drying 25 °C, 5 days, calcination 500 °C
39	CuO/SBA-15	5CuO/SBA-15[120]/ 25-5		
40	Co_3O_4/SBA-15	5Co_3O_4/SBA-15[120]/ 25-5		
41	SBA-15	SBA-15[140]	Catalytic support	Hydrothermal treatment 140 °C, 48 h, calcination 550 °C, desiccator $CaCl_2$
42	NiO/SBA-15	5NiO/SBA-15[140]/ 25-5	Catalytic precursor	5wt.%, drying 25 °C, 5 days, calcination 500 °C
43	CuO/SBA-15	5CuO/SBA-15[140]/ 25-5		
44	Co_3O_4/SBA-15	5Co_3O_4/SBA-15[140]/ 25-5		
45	Al-SBA-15	AS100	Catalytic support	pH adjusting method, Si/Al =100
46		AS50		pH adjusting method, Si/Al =50
47		AS20		pH adjusting method, Si/Al =20
48		AS10		pH adjusting method, Si/Al =10
49		AS5		pH adjusting method, Si/Al =5
50	NiO/Al-SBA-15	5NiO/AS50	Catalytic precursor	5wt.%, drying 25 °C, 5 days, calcination 500 °C
51	CuO/Al-SBA-15	5CuO/AS50		
52	Co_3O_4/Al-SBA-15	5Co_3O_4/AS50		
53	NiO/Al-SBA-15	5NiO/AS5		
54	CuO/Al-SBA-15	5CuO/AS5		
55	Co_3O_4/Al-SBA-15	5Co_3O_4/AS5		

In order to optimize the MDI method, the following parameters were investigated: (*i*) the texture of SBA-15, (*ii*) the drying time, (*iii*) pretreatment conditions after drying, (*iv*) the drying temperature, (*v*) the degree of loading with metals and (*vi*) the chemical composition of SBA-15 support.

O3/ Physico-chemical characterization of mono-metallic catalysts of M/SBA-15-type (M=Ni, Cu, Co)

After calcination, the oxidic forms of metallic catalysts obtained by MDI (MO/SBA-15) were systematically analyzed by various techniques such as ICP-OES, XRD at small and wide angles, nitrogen physisorption at -196 °C, TEM, *in-situ* XRD at wide angles and TPR aiming to study the effect of synthesis parameters on the properties of (oxidic)metallic NP on SBA-15 support: chemical composition, morpho-structural and textural properties, reducibility of metal precursors, metal-support interactions and thermostability of nanoparticles in oxidizing and reducing atmospheres, respectively (experimental details in Ungureanu et al.[4]). Metal forms were generally analyzed by *in-situ* XRD at wide angles and preliminarily by TEM and *in-situ* XPS.

Selection of the most significant results

(i) According to the literature,[4,5] the pore diameter of support (D_{pore}) can influence the average crystallite size of metallic oxides (MO) (d_{MO}) by their geometric confinement in primary mesopores (*effect of confinement*). In this respect, it was prepared a set of SBA-15 supports with calibrated D_{pore} in the range 7-10.9 nm and different fractions of micropores (Table 2). It was noted that the evolution of d_{MO} (calculated with Scherrer equation from diffractograms at wide angles) as a function of D_{pore} largely depends on the nature of deposited MO (Fig. 1A): (i) NiO/SBA-15: $d_{NiO} \sim D_{pore}$ (9.0 vs. 8.4 nm) only in the case of SBA-15[100] suggesting that this support is favorable for the confined crystallization of NiO NPs in primary mesopores; (ii) Co_3O_4/SBA-15: d_{Co3O4} (10.6-11.3 nm) is independent of D_{pore}.

Table 2. Textural properties of mesoporous support SBA-15 determined by nitrogen physisorption at -196 °C

Sample	S_{BET}, m^2/g	S_{micro}, m^2/g	V_{pore}, cm^3/g	V_{micro}, cm^3/g	D_{pore}, nm (NL-DFT)
SBA-15[60]	820	290	0.964	0.130	7.0
SBA-15[80]	714	208	0.962	0.096	8.0
SBA-15[100]	732	200	1.121	0.090	8.4
SBA-15[120]	548	92	1.059	0.03	9.0
SBA-15[140]	411	83	1.1	0.03	10.9

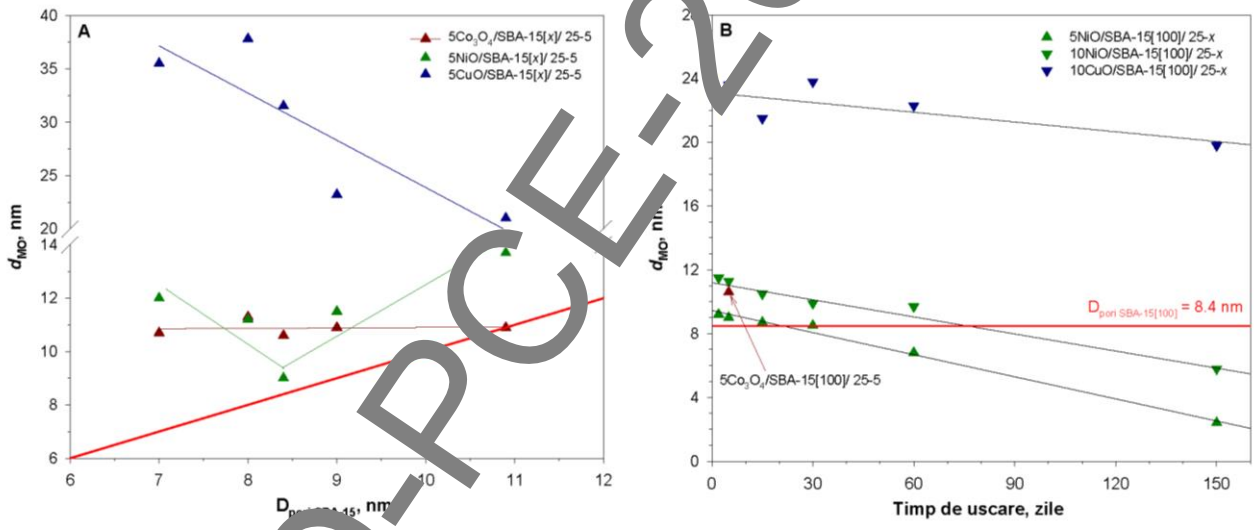

Fig. 1. Evolution of the average size of the crystallites of MO as function of: (A) - mesopores diameter of SBA-15, (B) - drying time.

For D_{pore} > 8 nm, d_{Co3O4} values are close to the size of mesopores, suggesting also the confined crystallization of Co_3O_4 NP in primary mesopores of supports with larger pores; (iii) CuO/SBA-15: d_{CuO} decreases with increasing D_{pore}. The size of crystallites (21-31.5 nm) is much larger than the dimensions of mesopores suggesting the transport of metal precursors to the external surface of the support grains and formation of bulky oxide particles. In line with these results, subsequent investigations involve only the support SBA-15[100] which probably has an optimal meso-/micro-structure for the dispersion of NP in mesopores in the form of confined oxide particles, and stabilized in both primary mesopores and secondary micropores/mesopores (they form a secondary pore system with variable pore diameters from 1.5 nm (supermicropores) to 4 nm (small mesopores) that interconnects the primary mesopores).[1]

(ii) From Fig. 1B, it can be observed that the drying time dramatically influences the dispersion of NiO nanoparticles deposited on SBA-15[100] by the MDI method (drying at 25 °C) irrespective of the degree of loading with metal (study (*v*): 5 and 10 wt.%), while the influence on the dispersion of CuO is negligible. Remarkably, in the case of samples 5NiO/SBA-15[100]/25-x, d_{NiO} decreases from ~ 8.5-9.2 nm (drying times 2-30 days; NPs dispersed and confined in mesopores) at 2.4 nm (drying time 150 days; NPs highly dispersed). In the case of samples with higher content of Ni, it was necessary a longer drying time in order to achieve high dispersion (150 days; d_{NiO} = 5.8 nm). These results can be explained by the fact that the increased drying times favor the advanced hydrolysis of $Ni(NO_3)_2 \cdot 6H_2O$ to $Ni(NO_3)_2 \cdot 2Ni(OH)_2$ (phases with low mobility) and the formation of 1:1 Ni phylosilicate (1:1 Ni PS).[4-6] Fig. 2 shows *in-situ* XRD diffractograms for samples dried at 25 °C and calcined at different temperatures: (i) it

is revealed the formation of NiO nanocrystals by the decomposition of $Ni(NO_3)_2 \cdot 2Ni(OH)_2$ (marked with *) in the range of temperatures 200 ÷ 300 °C, and (ii) irrespective of dispersion or metal loading degree, NiO NPs show high thermal stability to sintering under oxidative conditions (up to 600 °C).

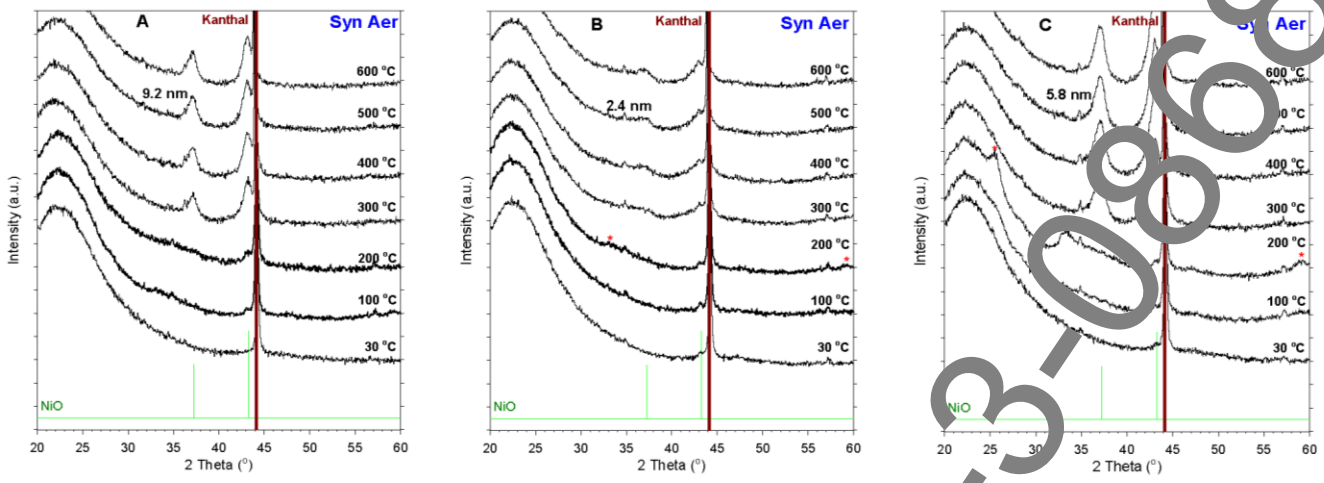

Fig. 2. *in-situ* XRD patterns for (A) 5NiO/SBA-15[100]/ 25-2, (B) 5NiO/SBA-15[100]/ 25-150 and (C) 10NiO/SBA-15[100]/ 25-150

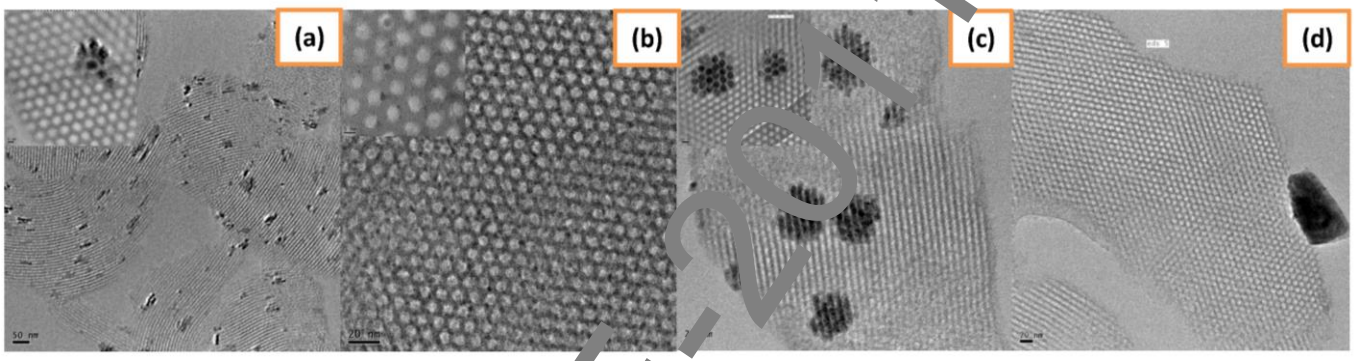

Fig. 3. TEM images for (a) 5NiO/SBA-15[100]/ 25-2, (b) 5NiO/SBA-15[100]/ 25-150, (c) $5Co_3O_4$/SBA-15[100]/ 25-5 and (d) 5CuO/SBA-15[100]/ 25-2 after calcination at 500 °C under stagnant air atmosphere.

Some representative TEM images for MO/SBA-15 samples are shown in Fig. 3: (*i*) bulky oxide aggregates (dimensions of 70-100 nm) on the external surface of SBA-15 grains were observed only for copper sample (image d);[7] (*ii*) 5NiO/SBA-15[100]/25-2 (see figure a): NiO nanoparticles appear well dispersed and uniformly distributed in the form of polycrystalline particles with nanorod-like morphology (diameters from 8-9 nm and variables length in the range 10 ÷ 50 nm) and which are confined in mesopores (sometimes, NPs which have crystallized inside of 2-3 adjacent mesopores form small nanobundle-like aggregates);[7] (iii) $5Co_3O_4$/SBA-15[100]/25-5 (see figure c): 6-7 nanorod-like polycrystalline nanoparticles of Co_3O_4 are associated as nanobundle-like aggregates which form specific patches of 60-100 nm diameter on support grains; (*iv*) 5NiO/SBA-15[100]/25-150 (see figure b): NiO crystals are highly dispersed in mesopores in the form of NPs with sizes of 2-3 nm.

(iii) Interesting results concerning the dispersion of the metallic nanoparticles of nickel were obtained when the calcination step was avoided (dried samples were directly subjected to reduction). The *in-situ* XRD diffractograms recorded under H_2/He flow for the Ni samples (5 wt.%), calcined and non-calcined, are comparatively presented in Figs. 4A and B. Notice that the direct reduction leads to NPs of Ni^0 undetectable by XRD, even after reduction at 600 °C, suggesting dimensions of particles smaller than 2 nm, as compared with the reduction of calcined form (note the diffraction peaks of Ni^0 (200) planes and less intense diffraction peaks after reduction at 550 °C). It should be noted that the calcined sample presents a low reducibility of NiO particles (the presence of specific diffraction peaks of NiO after reduction at 550 °C), in accordance with its TPR profile. Fig. 4 c shows that even in the case of higher loadings (10 wt.%), the direct reduction results in nano- sized particles of Ni (i.e., 2.4 nm). It could be mentioned that in the case of Cu containing materials the strategy of direct reduction was not effective in stabilizing the NPs, while in the case of Co-containing catalyst in-situ XRD analyses have shown that the reduction of calcined form at 750 °C leads to excellent results regarding the dispersion (~ 2.5 nm in size). Thus, it could be claimed that MDI method - drying at 25 °C - is extremely effective and versatile for obtaining (oxide)metal nanoparticles of Ni and Co highly dispersed and stable to sintering under severe oxidative and reductive conditions.

(iv) Another study was focused on the influence of drying temperature on the properties of metal nanoparticles. From Figure 4 it can be seen that regardless of the catalytic system, the temperature of 50 °C favors the formation of NPs with the lowest particle size, while the high temperatures lead to the lowest dispersions.

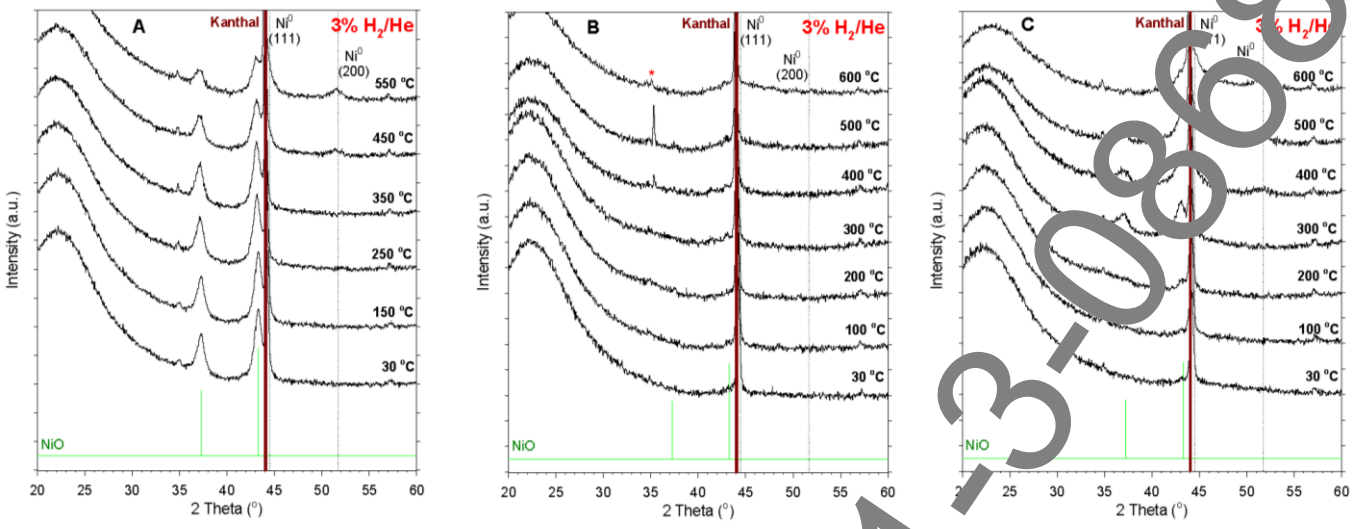

Fig. 4. *in situ* XRD patterns for (A) 5NiO/SBA-15[100]/ 25-2 calcined at 500 °C, (B) 5NiO/SBA-15[100]/ 25-2 non-calcined and (C) 10NiO/SBA-15[100]/ 25-2 non-calcined.

Interestingly to note the value d_{NiO} of 6.1 nm after drying at 50 °C for 3 days very close to d_{NiO} = 6.8 nm after drying at 25 °C for 60 days. It can thus assume that, at least in the case of nickel-based materials, the positive effect of the increasing of drying temperature at 50 °C, which is similar to that of the increasing of drying time (i.e., advanced hydrolysis to the metal hydroxy-nitrates and formation of phyllosilicates with role of nucleation/stabilization centers of oxide NPs and of metallic ones resulted from their reduction).

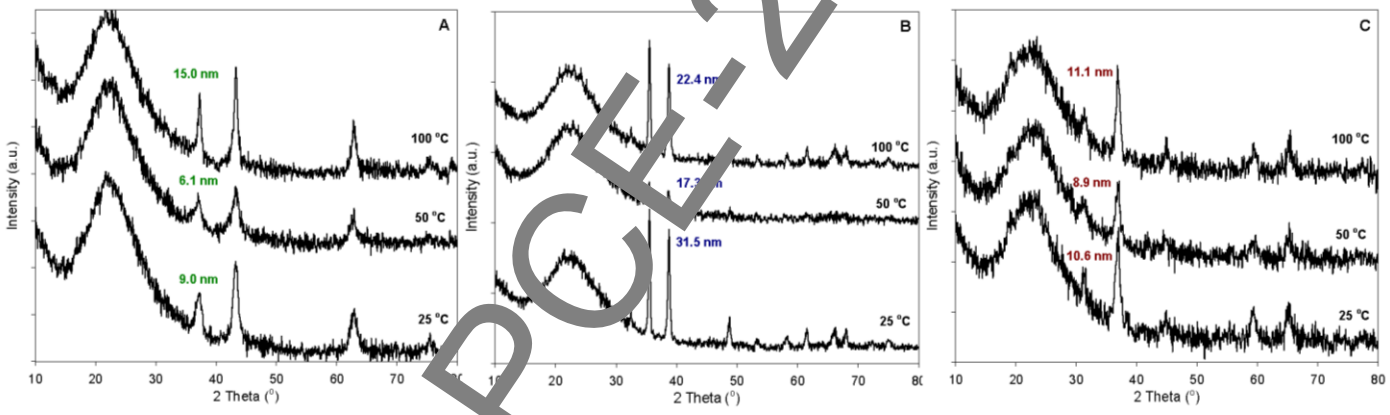

Fig. 5. DRX pentru (A) 5NiO/SBA-15[100]/ *x*-5, (B) 5CuO/SBA-15[100]/*x*-5 si (C) $5Co_3O_4$/SBA-15[100]/ *x*-5 calcinate la 500 °C

(vi) Study on the effect of chemical composition of SBA-15 support on dispersion of metal NPs has been started in the last phase of the project. Experiments, carried out to date, have assumed the use of two Al-SBA-15 materials as support with different Al content (AS50 and AS5). The results obtained on the MO/AS50 were in line with those obtained with MO/SBA-15, while the preliminary results obtained on MO/AS5 have shown a positive effect of the presence of aluminum on the dispersion of oxide nanoparticles as well as a negative effect on their reducibility, probably associated with the formation of some thermostable and hardly reducible phases of metal aluminates during calcination.

O5/ Evaluation of MDI method in comparison with conventional methods of preparation

To attain this objective, 12 other samples based on SBA-15[100] support (4 for each metal, 5 wt.%) have been prepared by wet impregnation (WI), incipient wetness impregnation (IWI), precipitation (P) and deposition by precipitation (DP) methods. After calcination, the obtained materials have been systematically analyzed by the above mentioned techniques and the results were compared with those obtained by MDI. For example, Fig. 6 illustrates that the method of preparation has a major influence on the structural, textural of and reducible properties of cobalt-based catalysts. Compared to the conventional methods of impregnation, the results show that the optimized MDI method leads to higher dispersion of metallic precursors due to confinement/stabilization of nanoparticles of Co_3O_4 in mesopores of support (d_{Co3O4} = 8.9 nm ~ D_{pore} = 8.4 nm), while methods based on precipitation lead to higher dispersion, yet affect the support mesoporosity due to basic conditions of synthesis. Similar trends were observed for Ni and Cu materials.

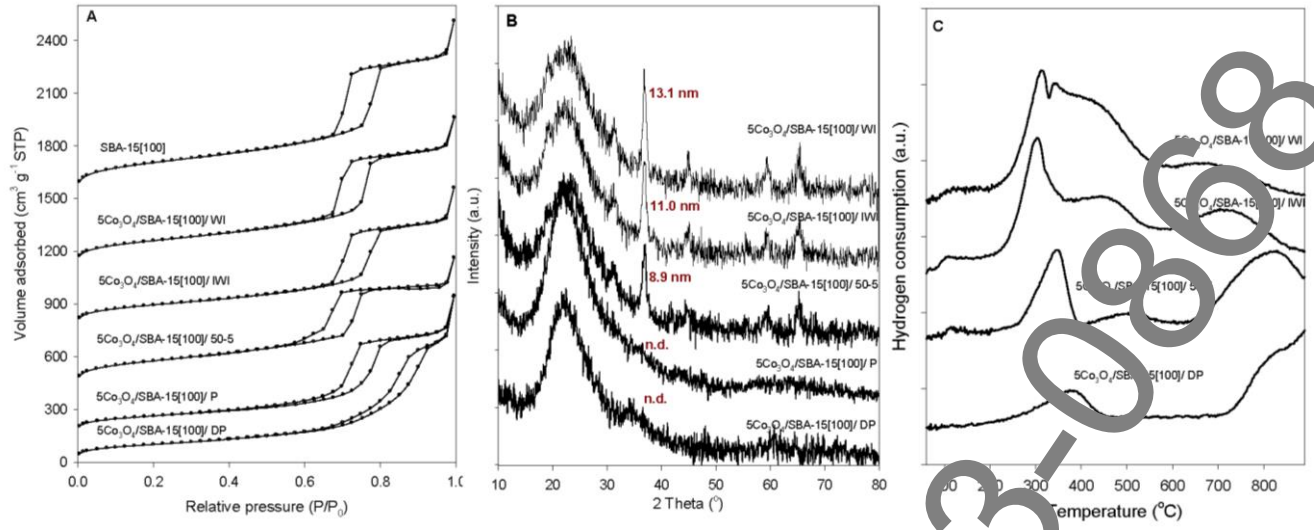

Fig. 6 (A) N_2 adsorption/desoption isotherms, (B) XRD patterns at high angles (C) TPR profiles for 5Co$_3$O$_4$/SBA-15[100] materials

O4/ Catalytic applications of metallic catalysts for chemoselective hydrogenation of cinnamaldehyde

The materials M/SBA-15 developed in this phase of the project have been tested in the liquid phase hydrogenation of cinnamaldehyde at 150 °C and atmospheric pressure. Some results are presented in Table 3, clearly illustrating the influence of several important factors (temperature, texture, drying time, chemical nature) and the neccesity to optimize the MDI method that proves to be very useful in obtaining efficient catalysts. Thus, following the influence of the temperature, it can be seen that the maximum catalytic activity is obtained for samples dried at 50 °C, regardless of the chemical nature of the active metal.

Table 3. Catalytic performances of M/SBA-15 materials derived from NiO/SBA-15, Co_3O_4/SBA-15 and CuO/SBA-15

No.	Sample	Code	Reaction time, min	X_{CNA}, % mole	S_{CNOL}, % mole	S_{HCNA}, % mole	S_{HCNOL}, % mole
1.	NiO/SBA-15 (reduction at 350 °C)	5NiO/SBA-15[100]/ 25-5	150	95	0.7	77.2	22.3
2.		**5NiO/SBA-15[100]/ 50-5**		**100**	**0.1**	**90.4**	**9.5**
3.		5NiO/SBA-15[100]/ 10[illegible]5		52	1.6	94.6	3.9
4.		**5NiO/SBA-15[100]/2[illegible]150**	90	**95.4**	**1.2**	**88.3**	**10.5**
5.		5NiO/SBA-15[10[illegible] DP	360	**0**	-	-	-
6.	Co_3O_4/SBA-15 (reduction at 500 °C)	5Co$_3$O$_4$/SBA-15[100][illegible]	1440	55.4	53.0	16.3	30.7
7.		**5Co$_3$O$_4$/SBA-15[100]/ 50**		**76.6**	**48.9**	**13.8**	**37.3**
8.		5Co$_3$O$_4$/SBA-[illegible]100]/ 100-5		64.4	43.6	18.0	38.4
9.		5Co$_3$O$_4$/SB[illegible]-15[100]/ D[illegible]		92.1	6.4	40.0	53.6
10.	CuO/SBA-15 (reduction at 350 °C)	5CuO/SBA-[illegible]5[100]/ 25-	360	2.0	37.6	23.6	38.8
11.		**5CuO/SBA-[illegible]100]/ 50-5**		**24.1**	**41.6**	**45.7**	**12.7**
12.		5CuO[illegible]15[100]/ 100-5		2.4	23.7	20.1	56.2
13.		5[illegible]O/SB[illegible]15[100]/ DP		43.2	38.7	44.6	16.8

According to the results of physico-chemical characterizations, this behavior is associated with smaller size of metal crystallites resulting in higher dispersion of active phases. In the case of nickel-based materials, it can be seen that similar results are obtained when the drying is run at 25 ° C, but for very long periods (150 days), that favors obtaining oxide NPs of very low dimensions (d_{NiO} = 2.4 nm and 5.8 nm, for 5 or 10 wt.%). The most interesting results from the series of materials synthesized by MDI method were obtained for sample Co_3O_4/SBA-15 dried at 50 °C (76.6% conversion and selectivity to CNOL of 48.9 %). When the samples obtained by MDI were compared with those prepared by traditional methods, it was found that: (*i*) MDI lead to more active catalysts than those obtained through WI and IWI; (ii) the MDI method leads to catalysts with higher selectivity to unsaturated alcohol than those obtained by precipitation methods (cobalt catalysts) or with similar selectivity (copper catalysts).

The original results of the studies have been the subjects of 6 communications at international scientific events, 1 published ISI paper[2] and 1 paper under evaluation[7] (see Annex at the report).

References

1. Galarneau, A.; Cambon, H.; Renzo, F. Di; Ryoo, R.; Choi, M.; Fajula, F. *New J. Chem.* **2003**, *27*, 73 - 79.
2. Ungureanu, A.; Dragoi, B.; Hulea, V.; Cacciaguerra, T.; Meloni, D.; Solinas, V; Dumitriu, E. *Microporous Mesoporous Mater.* **2012**, *163*, 51 - 64.
3. Sun, X.; Shi, Y.; Zhang, P.; Zheng, C.; Zheng, X.; Zhang, F.; Zhang, Y.; Guan, N.; Zhao, D.; Stucky, G.D. *J. Am. Chem. Soc.* **2011**, *133*, 14542 - 14545.
4. Ungureanu, A.; Dragoi, B.; Chirieac, A.; Royer, S.; Duprez, D.; Dumitriu, E. *J. Mater. Chem.* **2011**, *21*, 12529 - 12541.
5. Wolters, M.; van Grotel, L. J. W.; Eggenhuisen, T. M.; Sietsma, J.R.A.; de Jong, K.P.; de Jongh, P.E. *Cat. Today*, **2011**, *163*, 27 - 32.
6. Lewis, C.; Zheng, Z.X.; Che, M. *J. Phys. Chem.* **1993**, *97*, 5703-5712.
7. Ungureanu, A.; Dragoi, B.; Chirieac, A.; Ciotonea, C.; Royer, S.; Duprez, D.; Mamede, A.S.; Dumitriu, E. *ACS Appl. Mater. Interfaces*, submitted

Project leader,

Prof.dr.ing. Emil DUMITRIU